International Journal of Pharmaceutical and Bio-Medical Science

ISSN(print): 2767-827X, ISSN(online): 2767-830X

Volume 04 Issue 04 April 2024

Page No: 292-302

DOI: https://doi.org/10.47191/ijpbms/v4-i4-06, Impact Factor: 7.792

Formulation and Optimization of Intra Nasal Niosomal Gel of Kynurenic Acid: In Vitro in Vivo Characterization

Mounika Bodige[1], Rakesh Kumar Jat[2], Ananda Kumar Chettupalli[1]

Research scholar, Department of Pharmaceutical sciences, Shri Jagdish Prasad Jhabarmal Tibrewala University Chudela Jhunjhunu Rajasthan- 333001.

[1]Assistant professor Department of pharmaceutical sciences Vignan Institute of pharmaceutical sciences Vignan hills, Near Ramoji film city, Deshmukhi, Yadadri Bhuvanagiri- 508284.

[1]Department of pharmaceutical sciences, Center for Nanomedicine, Anurag University, Hyderabad, Telangana-500088.

[2]Department of pharmaceutical sciences, Institute of Pharmacy Shri Jagdish Prasad Jhabarmal Tibrewala University Chudela Jhunjhunu Rajasthan- 333001.

ABSTRACT

Kynurenic acid's (KNA) inability to cross the blood brain barrier (BBB) severely limits its usage as a neuroprotective drug, despite the fact that it may have significant therapeutic effects in neurological illnesses. Drug delivery devices are one of the new avenues we're exploring as a means for KNA to enter the brain. Due to its low absorption when taken orally, medication formulation faces a significant hurdle. Here, nasal drug delivery has emerged as a popular alternate method for increasing medication bioavailability. In light of this, the current investigation set out to increase KNA bioavailability by means of an intranasal formulation based on niosomal technology. Rapid onset and evasion of first-pass metabolism are both offered by the nasal route, whereas niosomes protect hydrophilic medicines inside their core. For the purpose of determining entrapment efficiency, particle size, and in vitro drug release, niosomes were synthesized by combining lipid, nonionic surfactant, and cholesterol in distinct ratios. With a vesicle size of 248.51±1.54nm, the optimized niosomal formulation demonstrated a superior drug content (DC) of 98216±0.11% and an entrapment efficiency (EE) of 89.23±0.35. The formulation also contained cholesterol in an equal proportion (1:1). A value of 24 minutes was shown in the in vitro drug diffusion testing, indicating that the formulation exhibited prolonged activity. Gelation occurred at 37 ºC, which is the body's physiological temperature, and the optimum in situ gel, which contained 1:2 carbopol 934 and benzalkonium chloride, had a t90 value of 24 hours, indicating prolonged activity. In comparison to KNA oral suspension, the results showed that the KNA-loaded niosomal gel had a much higher relative bioavailability and improved drug penetration through the nasal mucosa.

KEYWORDS: Drug release in vitro, kynurenic acid, niosomes, particle size, entrapment efficiency.

ARTICLE DETAILS

Published On:
11 April 2024

Available on:
https://ijpbms.com/

INTRODUCTION

The nasal mucosa has several advantages over other possible routes of drug delivery, including a wide surface area, a porous endothelium membrane, a high total blood flow, the ability to bypass first-pass metabolism, and easy accessibility. For medications degradable by enzymes, it has become a non-invasive alternate approach. One downside of nasal delivery is the short residence duration caused by mucociliary clearance [1-3]. We have devised a delivery system based on the concept of in situ gel formation to increase the residence period of topically administered medications in liquid form. The polymers used to make these delivery systems undergo phase shifts as a result of the physicochemical changes occurring in their local surroundings. Injecting the liquid delivery systems into the nasal mucosa, mouth, or any other physiological milieu causes them to solidify into a gel. To

further circumvent the mucociliary clearance process, these formulations make use of bioadhesive excipients, which cling to the mucosal membrane and extend the residence period in the nasal cavity. The nasal medication absorption and bioavailability are enhanced, and the drug undergoes rapid first pass metabolism, as a result [4].

To address the issue of pharmaceutical medications' low bioavailability, nano-sized drug delivery systems have been the subject of much research for the last several decades. There have been numerous applications for nanoparticulate delivery methods, such as niosomes, dendrimers, solid lipid nanoparticles, micelles, liposomes, and polymeric nanoparticles. Vesicular carriers offered other advantages, like protecting active compounds from chemical and enzymatic degradation and potentially extending the duration of medication distribution in the bloodstream [5-9].

One of the greatest nano-vesicles that may circumvent the nasal route's ciliary clearance constraint is niosomes (NSMs). Hydrophilic medications can be housed in NSM with remarkable stability and efficacy [6]. Similarly to liposomes, niosomes are self-assembled vesicles with one or more lamellae that have been created by hydrating synthetic nonionic surfactants and adding cholesterol or other lipid surfactants [7]. They are less harmful and can transport medications to the desired location because they are not ionic. The medicine is encased in niosomes, which improves its stability, bioavailability, and mucosal penetration while avoiding some of the problems with liposomes [8–12]. A stable formulation for nasal medication administration was prepared using the dual capabilities of niosomes and in situ gels.

The tryptophan metabolite kynurenic acid (KYNA) is produced enzymatically through the kynurenine pathway. Enzymes that convert tryptophan to formyl kynurenine, known as tryptophan 2, 3-dioxygenase (TDO) and indoleamine 2, 3-dioxygenase (IDO), catalyze the initial step of the pathways. IDO is an enzyme that can be activated by cytokines outside of the liver, whereas TDO is mostly expressed in the liver. After the first step in kynurenine production is completed, amidase catalyzes the second step. Niacinamide adenosine dinucleotide (NAD+) is the primary byproduct of kynurenine metabolism. From kynurenine-by-kynurenine aminotransferase, another physiologically active molecule called KYNA is produced [14, 15]. The presence of KYNA in urine was initially shown by Liebig.3 But it wasn't until the 1980s and 1990s that researchers proved KYNA is an antagonist of ionotropic glutamate receptors; before to that, the molecule had not been extensively studied. Based on this, scientists have concluded that KYNA must exist in the human brain. The function of KYNA in CNS physiology and pathology has been the subject of a great deal of research. Research on peripheral KYNA has grown in prominence due to the low concentration of KYNA in the brain and its inability to cross the blood-brain barrier [16].

New knowledge that may pave the way for in

MATERILAS & METHODS

Materials

kynurenic acid was purchased from Qingdao Sigma Chemical Co., Ltd. (Qingdao, China). Span® 80 (sorbitan trioleate) and cholesterol were purchased from Sigma-Aldrich Co. (St Louis, MO, USA). Ethanol was purchased from EMD Millipore (Billerica, MA, USA). All other reagents and chemicals were of analytical grade

Methods

Investigations of the chosen medicine's solubility conducted prior to formulation:

The medicine of choice was tested for solubility in distilled water and phosphate buffer at a pH of 7.4 according to the established procedure [17]. To make a saturated solution, we measured out the aforementioned solvents individually and mixed them with an excess quantity of the medication of choice in a glass beaker. To help get the undissolved drug particles into equilibrium, the solution was shook every so often. After a day, the filtered drug solution was taken out and diluted with different solvents in a certain order. The concentration was then determined using a spectrophotometer. Readings were taken three times and averaged [18].

Melting point determination:

A little amount of the drug was placed in a capillary tube with one end closed. It was then placed in Thiel's melting point device and the temperature at which the drug melted was recorded [19,20]. Readings were taken three times and averaged.

Partition coefficient determination:

An n-octanol solution containing 1 mg/ml of the medication was made. 25 ml of this solution was transferred to a separating funnel and mixed with an equivalent volume of phosphate buffer (aqueous phase) with a pH of 7.4 for 10 minutes. The mixture was then left to stand for two hours. It was then centrifuged at 2000 rpm to separate the organic phase and the aqueous phase 50. The drug concentration was measured using a UV spectrophotometer in both phases. One way to determine the partition coefficient was to compare the drug concentration in the aqueous phase with that in the n-octanol phase [21-22].

Drug excipients compatibility studies:

Fourier Transform Infrared (FTIR) Spectroscopy:

Infrared spectroscopy was used to acquire the samples' Fourier transform infrared (FTIR) spectra by means of the KBr disk method [23]. Various mixtures were created and analyzed using Fourier transform infrared spectroscopy (FTIR). These mixtures included the pure drug sumatriptan, a physical mixture of sumatriptan and carbopol 940P, and some liquid paraffin. An equivalent weight of dried potassium bromide and approximately 2-3 mg of sample were crushed to create a KBr disk. The spectra of the samples were scanned with a resolution of 4 cm-1, spanning from 400 to 4000 cm−1.

Preparation of Kynureic acid (KYA) niosomes

The preparation of KYA niosomes was carried out using a slightly modified version of a previously described approach [24]. To summarize, in a round-bottom flask, 10 mL of ethanol was added to mix with precisely measured doses of KYA (10 mg), cholesterol (CH, 5-30 mg), and Span® 80. After that, the organic solvent was removed from the ethanolic solution by evaporation under reduced pressure (R-200; BÜCHI Labortechnik AG, Flawil, Switzerland) at 45 ◦C for 2 hours. The niosmal dry film that had developed on the inside of the flask was hydrated using 10 mL of phosphate buffer under normal pressure after the solvent had been completely removed; the experimental design dictated the hydration time and pH of the buffer. The created niosomal suspension was sonicated for 60 seconds with a 40-amp, 750-watt, 20-kilohertz Sonics Vibra Cell tapered microtip (Sonics & Materials Inc., Newtown, CT, USA) in order to reduce the size of the vesicles. Before doing any more research, the niosomal dispersion was left at 4 ◦C overnight to mature [25].

Table 1: Formulation of KYA niosomes

Drug/ Excipients	KYA-1	KYA-2	KYA-3	KYA-4	KYA-5	KYA-6
KYA	10	10	10	10	10	10
Cholesteol	5	10	15	20	20	30
Soyalecithin	5	5	5	5	5	5
Methanol	1	1	1	1	1	1
Chloroform	4	4	4	4	4	4
Tween 80	2	2	2	2	2	2

Characterization of KYA niosomes

Morphology and size

Niosomes were analyzed by way of transmission electron microscopy (TEM) at an accelerating voltage of 80 kV (H-7500, Hitachi, Tokyo, Japan). After allowing the produced niosome to attach to a carbon-coated copper grid for approximately two minutes, any excess sample was filtered out using filter paper. The carbon grid was dyed with a 2% (w/v) phosphotungstic acid droplet. Utilizing filter paper, any residual stain was eradicated. After allowing the samples to air dry, we looked at the colored niosome thin coating [26]. Zetasizer ZEN3600 dynamic light scattering (DLS) analysis was used to determine the average particle size and size distribution of each niosomal formula [27]. The instrument was developed by Malvern Instruments Limited of Malvern, UK.

Zeta potential and particle size measurement

We used a Zetasizer Nano ZS from Malvern Instruments in Malvern, UK, to measure the particle size (PS), zeta potential (ZP), and polydispersity index (PDI) of NF-loaded niosomes. Distilled water was used to thin the niosome suspensions before examination. Three separate measurements were taken to ensure accuracy [28].

Determination of % entrapment efficiency

Centrifugation was used to obtain the percent entrapment efficiency (%EE) of the niosomal solution. REMI Instruments Division, Vasai, India, provided the freshly prepared niosomal suspension (5 ml), which was centrifuged at 9000 rpm for 45 minutes. After removing the supernatant, distilled water was used to dilute the mixture. Using a UV spectrophotometer (Shimadzu), we measured the amount of free medication in the supernatant layer. The following equation was then used to assess the drug's entrapment efficiency [29].

$$\text{Entrapment efficiency (\%)} = \frac{\textit{Initial amount of drug added} - \textit{Drug amount in supernatant}}{\textit{Initial amount of drug added}}$$

Optimization of KYA Niosomes

The optimal formulation of KYA niosomes, with reduced vesicle size and increased drug entrapment, was predicted by applying numerical optimization and computing desirability. The optimization approach was carried out using the Design-Expert software (Version 12; Stat-Ease Inc., Minneapolis, MN, USA) (Pharmaceutics 2020, 12, 485 5 of 23). We made sure the amounts of the recommended optimal variables and the projected responses were valid by preparing and testing the optimal formulation three times.

Characterization of Optimized KYANiosomes

Optimal KYA niosome structures were studied by means of transmission electron microscopy (TEM) with an operating voltage of 200 KV (Philips XL30, Eindhoven, Netherlands). The adsorption process began with a 2-minute placement of a carbon-coated grid onto a sample of diluted niosomal dispersion. To prepare the adsorbed niosomes for imaging, they were first negatively stained with uranyl acetate and then allowed to air dry. The enhanced KYA niosomes' physical stability was investigated by subjecting them to three freeze-thaw cycles, ranging from -20 ◦C to +25 ◦C. Statistical analysis was performed using the paired student t-test at $P < 0.05$ to compare the vesicle size and EE % of the formulation before and after the cycles [30].

Preparation of KYA Niosomal In Situ Intra-Nasal Gel

The 0.7% w/v gellan gum dispersion was made by swirling a boric acid/borax buffer (pH 7.4) while it was sprinkled over at 80 ◦C. Until a clean dispersion was achieved, the liquid was agitated continually. To achieve a KYA concentration of 10 mg/g, tailored KYA niosomes were added to a gellan gum dispersion after cooling. Once

prepared, the niosomal-loaded in situ gel was left at 4 ◦C for 12 hours prior to evaluation in order to release any air bubbles that had become trapped therein. To ensure fair comparison, a control was also constructed using raw KYA loaded in situ gel at the same concentration. Before and after adding simulated nasal fluid (SNF), the viscosity and gelation of the generated KYA niosomal in situ nasal gel formulation were tested [31]. Middleborough, Massachusetts, USA's Brookfield Engineering Laboratories provided the digital viscometer used to measure the viscosity. At 10 rpm 30 seconds before and after gelation, the apparent viscosity was measured.

Table 2. Composition of Carbopol 934P gel preparation.

Composition	Formulation Code					
	G1	G2	G3	G4	G5	G6
Carbopol 934P (%w/w)	0.2	0.5	0.8	1	1.2	1.5
KYA-Niosomes (mL) (Drug equivalent to 5 mg)	10	10	10	10	10	10
Benzalkonium chloride (%)	0.1	0.1	0.1	0.1	0.1	0.1
TEA (%)	2	2	2	2	2	2
Water	Q. S	Q. S	Q. S	Q. S	Q. S	Q. S

Ex Vivo Permeation

An ex vivo permeation investigation was conducted using fresh excised bovine nasal mucosa acquired from the abattoir and an automated Franz diffusion cell vertical diffusion cell test system (Microette Plus Hanson research, CA, USA). In order to delipidize the mucosa, a mixture of chloroform and methanol was utilized for 45 minutes [32]. An effective diffusional area of 1.76 cm2 was achieved by mounting mucosal samples between the two chambers of the diffusion cell. In the donor chamber, the mucosa was directly contacted by either an optimized KYA niosomal loaded in situ gel (0.1 g) or a control raw KYA loaded gel. Seven milliliters of simulated nasal fluid (SNF) with a pH of 6.5 was used as a diffusion medium in the receptor chamber. According to reference [33], the SNF had 7.45 mg/mL of sodium chloride, 1.29 mg/mL of potassium chloride, and 0.32 mg/mL of calcium chloride dioxide. The agitation rate was adjusted at 400 rpm and the temperature was kept at 35◦C ± 0.5◦C during the entire trial [34, 35]. Aliquots of 1.5 mL were removed and replaced with new diffusion media at prearranged intervals of 0.5, 1, 2, 4, 6, and 8 hours. For this analysis, we used HPLC-UV diode array detection, a technique developed for use in professional laboratory work. Time was used to depict the average cumulative amount of KYA that infiltrated the mucosal surface per unit surface area (µg/cm2). Afterwards, the coefficients for diffusion (D), permeability (Pc), and steady-state flow (Jss; µg/cm2.h) were determined.

RESULTS

Solubility:

The equilibrium solubility method was used to conduct KNA solubility investigations in various solvents using a cyclone mixer (REMI CM 101, India). Research on the drug's solubility in various solvents and buffer solutions is displayed in the table. Distilled water had a solubility of 0.59 ± 0.23 mg/mL for KNA, while ethanol had a solubility of 25.36±0.12 mg/mL at 250C, and polyethylene glycols have a higher solubility. The drug's solubility investigation found that it is soluble in methanol but practically insoluble in water. There is a reported solubility of 0.8 mg/mL of KNA in water.

Partition coefficient determination

Experimental evidence such as lipid membrane affinity, interactions with hydrophobic domains of proteins, and capacity to penetrate the blood-brain barrier support the idea that KNA is hydrophobic, according to expected values of log P ranging from 2.07 ± 0.06 to 2.31± 0.02. As previously stated, KNA is easily detectable and quantifiable due to its spectral properties. It was determined that the log P value of KNA in the octanol:water solution was 2.09 ± 0.03. The obtained log P value agreed with the stated value of around 3.0. Drugs with a log P greater than 1 are hydrophobic..

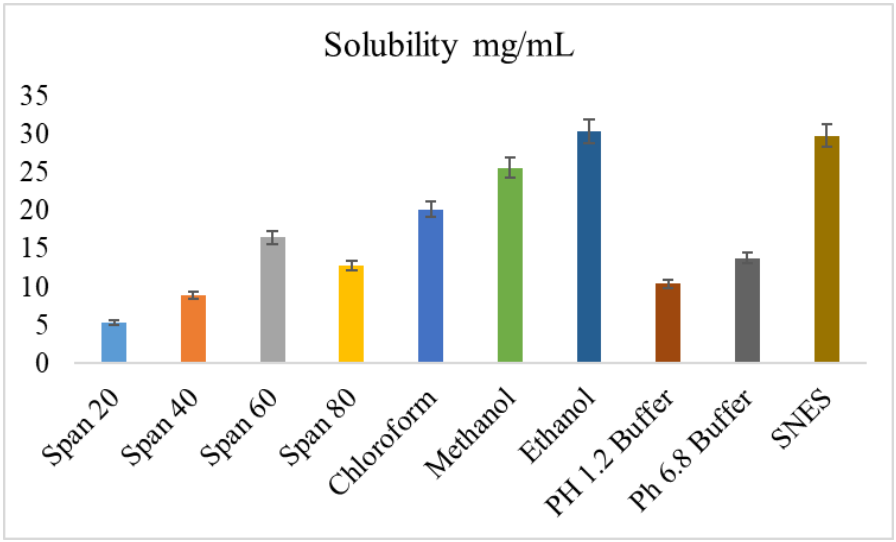

Figure 1: Solubility determination of different solvents and buffer medium

Entrapment efficiency:

When studying niosomal vesicles, the entrapment efficiency is a crucial metric to consider. This study found that KYA has an encapsulation effectiveness of 89.23±0.35% within niosomal vesicles. The drug's hydrophilic properties may explain why the % EE is quite low. The fact that the volume of water in the aqueous core of the vesicle is relatively lower than that which leaves outside the bilayered vesicle is well known during the passive loading of water-soluble medicines into these vesicles. medicines that are more hydrophilic typically have a lower % EE compared to medicines that are less water-soluble.

Table 2: Characterization of KNA loaded Niosomal Formulations

F. Code	Particle size	%EE	PDI	ZetaPotential
KYA-1	326.51±2.36	76.84±0.24	0.321±0.02	-15.26±0.13
KYA-2	248.51±1.54	89.23±0.35	0.126±0.05	-24.85±0.26
KYA-3	269.71±3.06	80.46±0.16	0.259±0.06	-19.86±0.34
KYA-4	302.61±5.13	75.16±0.85	0.354±0.03	-20.53±1.12
KYA-5	336.28±2.08	69.52±0.94	0.218±0.01	-22.35±0.95
KYA-6	321.04±3.64	72.84±0.26	0.136±0.02	-16.49±0.64

Drug excipient interaction studies:

The compatibility of KYA with various components of the niosomal formulation was examined using DSC. The melting temperatures of cholesterol and Tween 80 were 149 and 54 ˚C, respectively, where their endothermic peaks were seen. The thermogram of pure KYA exhibited a distinct sharp peak at 115 ˚C, which is the same as the melting point of KYA. The improved KYA niosomes were interesting because they lacked the drug's usual peak. This indicates that the medication is appropriately enclosed within niosomal vesicles.

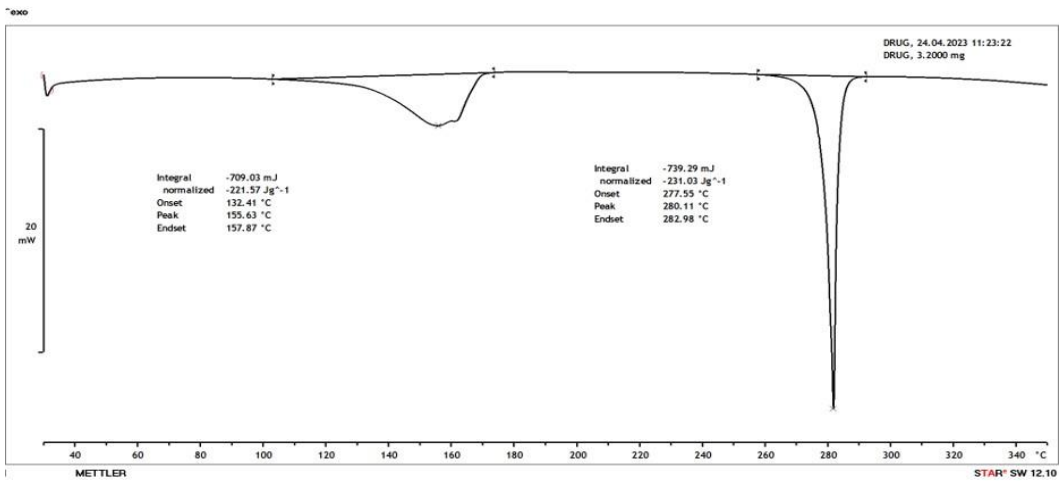

Figure 2: DSC thermogram of Pure drug (KYA)

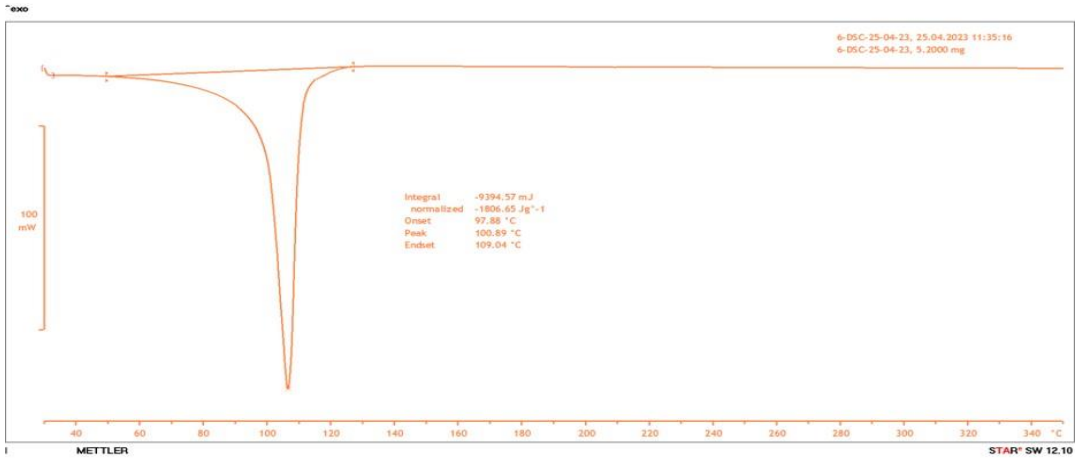

Figure 3: DSC thermogram of optimized niosomal formulation (KYA-2)

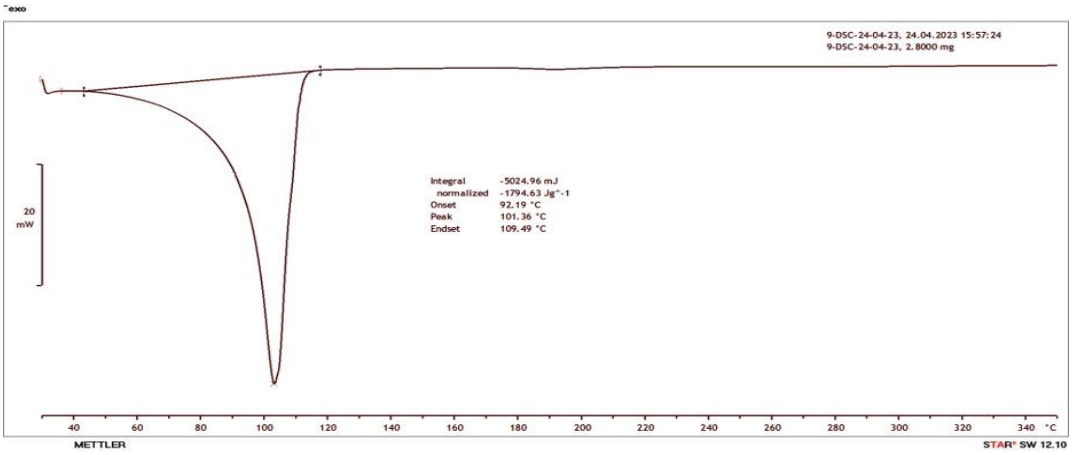

Figure 4: DSC thrmogram of optimized Niosomal insitugel formulation (KYAG)

Particle size analysis and polydispersity index (PDI):

A critical parameter in topical distribution that controls nanocarrier penetration across the skin barrier is the particle size of nanovesicles. The optimized KYA niosomes were shown to be suitable for cutaneous administration, as their vesicle size was 248.51±1.54 nm. A review of the gel formulations including KYA-loaded niosomes :

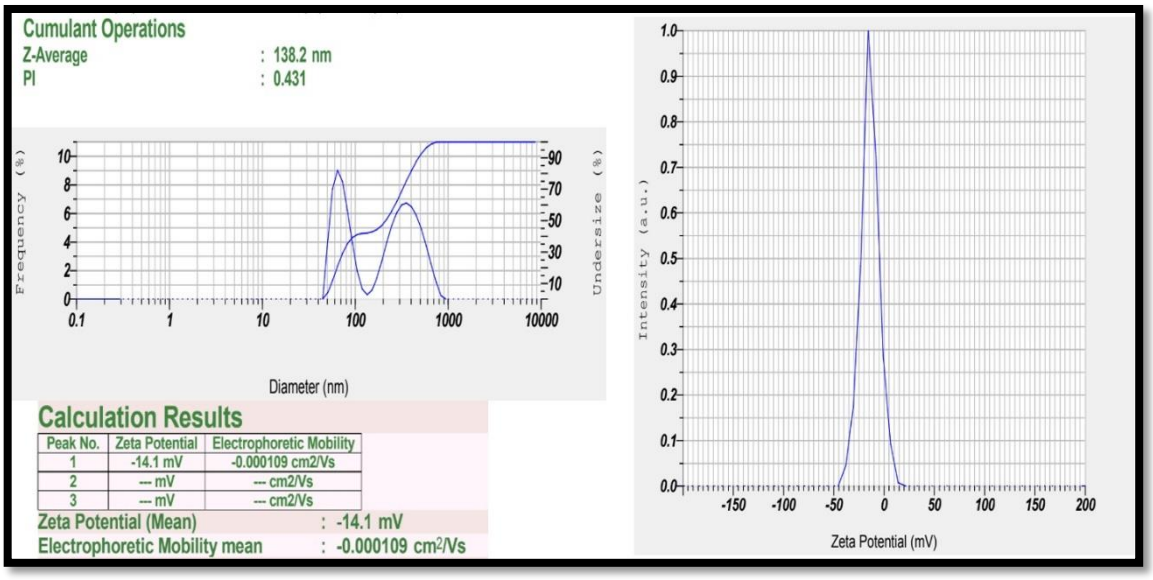

Figure 5: Particle size and zeta potential of KNA-loaded niosomes

Zeta potential

We used Zetasizer to check the niosomal formulation's zeta potential and move on with our experiments. Based on the findings presented in Table 2, it is evident that KYA-1 had the highest zeta potential (-15.26±0.13) and KYA-2 had the lowest (-24.85±0.26). Possible causes include an increase in the surfactant's hydrophilicity and a corresponding rise in its zeta potential, as mentioned in the works of Balakrishnana et al. and Sambhakar et al. 4 Niosomes had a zeta potential ranging from around -10 mV to -30 mV, indicating that they were negatively charged.

pH and Viscosity of gel:

A pH meter (Mettler Toledo, Switzerland) was used to measure the pH of the niosomal gels. The meter was calibrated using a standard buffer before the study. At 25 °C, the gel's viscosity was measured using a viscometer with a spindle speed of 0.3 rpm.

Spreadability test:

An established procedure was used to examine the KYA loaded niosomal gel's spreadability. One glass plate was used for analysis after 1 gram of niosomal gel was placed in a 1.2 cm pre-marked area on the first plate. A weight of 73 g was applied to the top glass plate and left there for 1 minute. Since the test's recording of the gel dispersion was dependent on the weight on top of the plate, this was the case.

Extrudability:

A customized tester was used to assess the extrudability of KYA loaded niosomal gel compositions. The aluminum tube was filled with 15 g of the prepared niosomal formulation and kept in position with the help of the plunger. After that, the gel was forcibly extruded from the tube by applying a pressure of 1 kg/cm2 for 30 seconds. After that, it was weighed and measured again at three evenly spaced points down the tube.

Table 2. Composition of niosomal insitu nasal gel formulation of KNA.

F code	Carbopol 934P (%w/v)	HPMC K4M (%w/v)	Benzalkonium Chloride (% w/v)	Gelling Time* (mins)	Gelling Capacity *	Viscocity (mPa s at 20 rpm)*	
						At pH 5	At pH 6
F1	0.5	0.2	1	5.39±0.26	-	1534±0.24	5763±0.23
F2	0.5	0.4	1	6.97±0.13	+	1689±0.36	6214±0.16
F3	0.5	0.6	1	9.58±0.21	++	1943±0.51	6983±0.25
F4	1	0.2	1	5.68±0.34	++	1827±0.29	7298±0.34
F5	1	0.4	1	4.25±0.12	+++	2146±0.35	7946±0.39
F6	1	0.6	1	3.26±0.25	++	2863±0.48	8236±0.42
F7	1.5	0.2	1	6.84±0.31	+++	1452±0.25	6251±0.51
F8	1.5	0.4	1	11.42±0.16	++	1695±0.16	7593±0.26
F9	1.5	0.6	1	13.02±0.13	++	1873±0.32	7941±0.75

* Total ± standard deviation (n=3) Just a quick note: - indicates no gelation, + indicates rapid dissolution after a few minutes of gelation, ++ indicates immediate gelation and stays for a few hours, and +++ indicates immediate gelation and stays for a long time.**Surface Morphological studies:**

The surface morphology of both blank and FAR-loaded niosomes was examined using Atomic Force Microscopy (AFM, Nanosurf C3000, Switzerland). The mica plate was treated with 10 microliters of niosome solution, allowed to air dry, and then analyzed using tapping mode. Both tests made use of low-stress silicon nitride cantilevers. We used a Transmission Electron Microscopy (TEM) system (Tecnai 20, Philips, Holland) with an accelerating voltage of 200 kV to look at the optimized KYA loaded niosomes. Phosphotungstic acid was used to color the niosomes in the samples, which were thoroughly mixed. The samples were allowed to air dry after being delicately placed over a copper grid covered with carbon. After that, the grids were attached to the device, and images were captured at different magnifications.

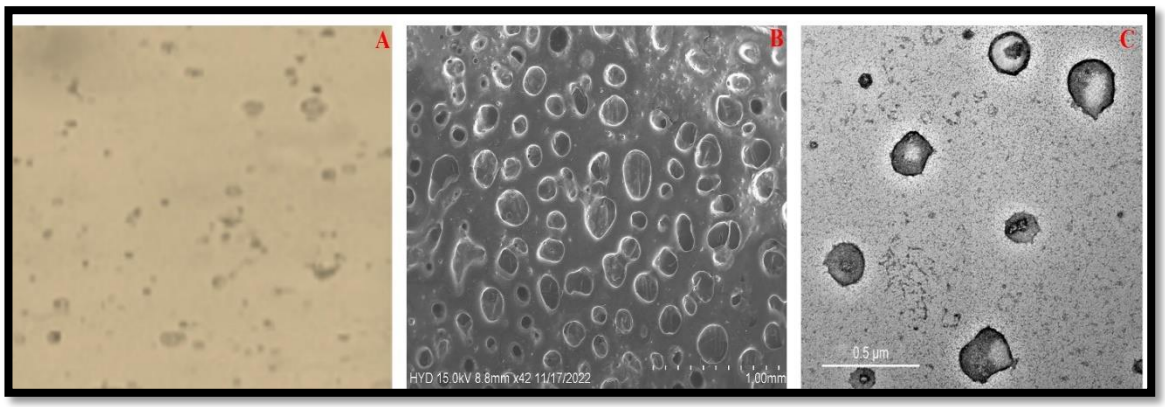

Figure 6: A). Optical microscopy, B) SEM and C) TEM of niosomes.

In vitro release study :

A 100 ml beaker containing phosphate buffer saline diffusion medium with a pH of 7.4 was used to appropriately suspend the niosomal formulation, which was taken in a 5 cm length dialysis membrane. The medium's temperature was kept at 37±0.5°C. A magnetic stirrer was used to continuously mix the substance. The volume of the diffusion medium was kept constant at 100 ml by withdrawing 1 ml of sample and replacing it with 1 ml of fresh buffer every hour. The diluted samples were prepared up to 10 mL in volume using phosphate buffer with a pH of 6.8 as the solvent. Spectrophotometric measurements were taken at 260 nm for the samples [36].

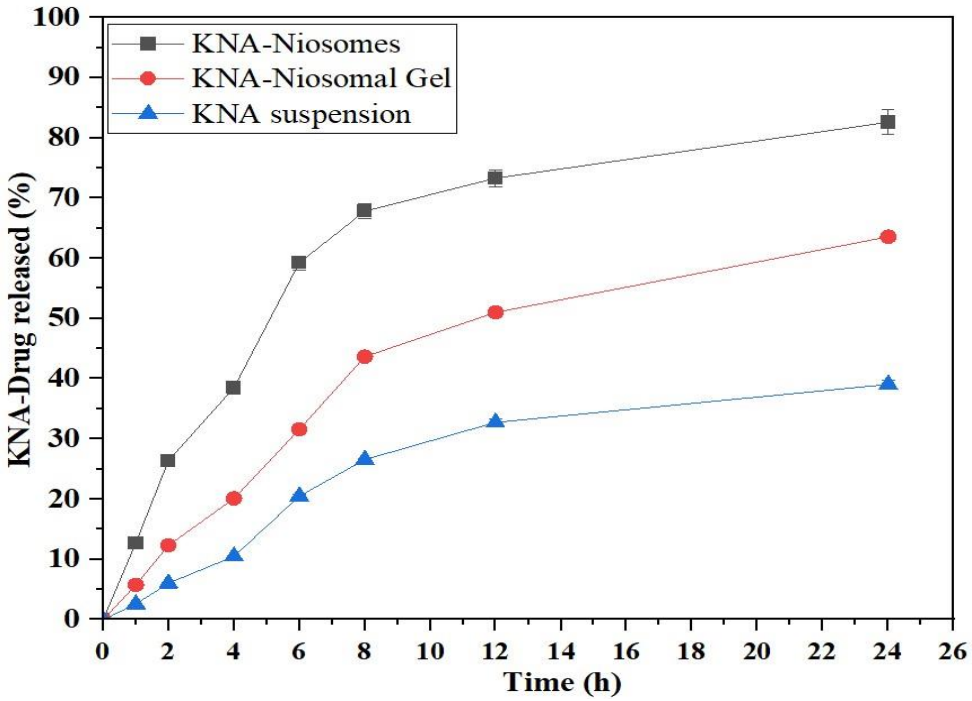

Figure 7: Invitro drug release studies of optimized KYA-Niosomes and niosomal gel

Characterization and Ex Vivo Permeation of KYA Niosomal In Situ Gel :

A suitable viscosity of 117 ± 0.98 cps was displayed by the in situ gel formulation containing improved KYA niosomes, allowing for easy instillation into the nose. The increased gelling factor shows that the formulation went from a viscous solution to a gel after being exposed to SNF. The gelation process raised the formulation's viscosity to 435 ± 1.78 cps. A possible explanation for this gelation, which is beneficial for the drug's retention in the nasal cavity, is the cross-linking activity of SNF cations on the helices of gellan gum.When comparing KYA niosomal in situ nasal gel to raw KYA in situ gel, an ex vivo permeation investigation was conducted using simulated nasal fluid with a pH of 6.5. Figure shows the cumulative amount of ex vivo KYA that permeated through the freshly excised bovine nasal mucosa over time.

The permeation profile clearly demonstrates that the in situ gel containing optimized KYA niosomes improved the total amount of permeated KYA (85.19% ± 4.59) in comparison to the control gel containing raw KYA (46.17% ± 5.10). Either the drug or the drug-loaded niosomes could have been integrated into the in situ gelling matrix that forms when

exposed to the SNF, explaining the slow release that both formulations exhibited. The calculated diffusion and permeability coefficients of the KYA niosomal gel were noticeably greater than those of the control gel, as shown by an unpaired Student-t test with a p-value of less than 0.05. Furthermore, when contrasted with the raw KYA gel, the niosomal gel displayed an enhancement factor of 1.84. One possible explanation for the increased KYA penetration from the niosomal in situ gel is that the niosomes make the medication more soluble. Cholesterol and surfactant establish hydrogen bonds due to their amphiphilic natures; this increases the solubility and content of KYA within the niosomal core, which in turn facilitates drug release.Another factor that could boost the drug's diffusion over the nasal mucosa is the inclusion of a nonionic surfactant (Span®), which acts as a permeation enhancer, together with the lipidic property and nano-size of the niosomes [37].

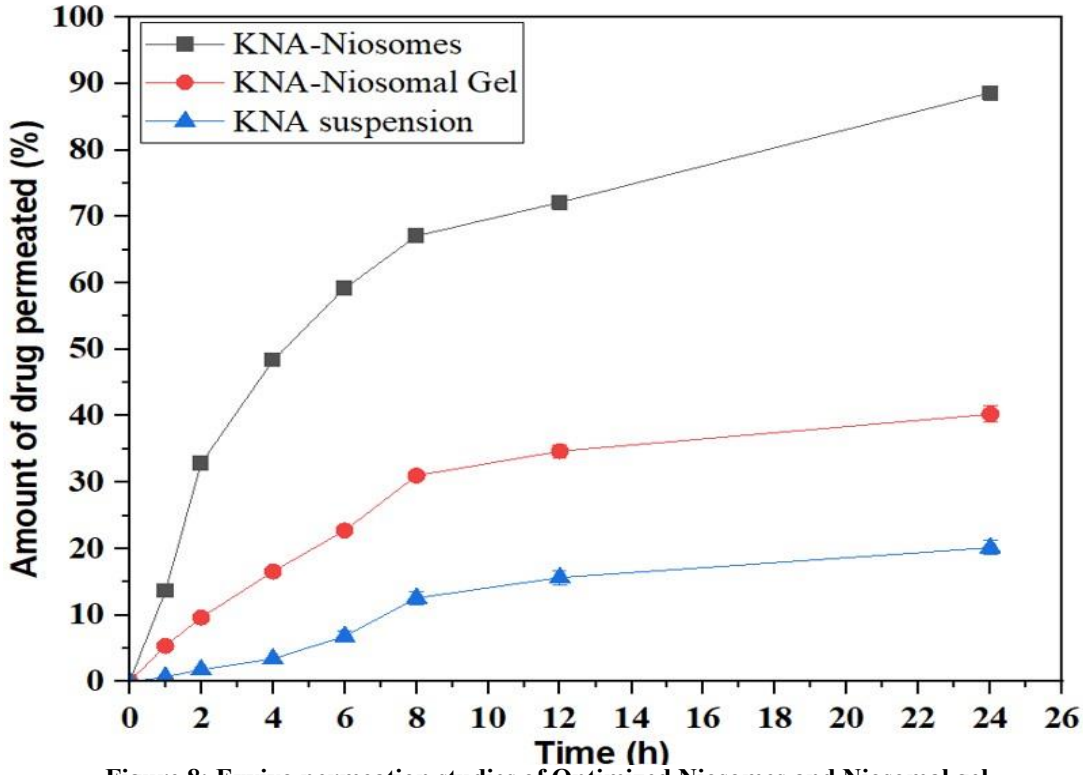

Figure 8: Exvivo permeation studies of Optimized Niosomes and Niosomal gel

CONCLUSION

The created vesicles effectively contained the examined medication, KNA, at their center. The drug release rate was prolonged and KNA permeability across nasal mucosa was greatly improved by the niosomes and niosomal gel that were developed. Research conducted in living organisms has demonstrated that niosomeal gel has the potential to enhance medication bioavailability, leading to a decrease in the effective dose that needs to be administered. Our results provide credence to the idea that intranasal distribution of KNA-loaded niosomal gel might be an effective substitute for the more traditional oral route by avoiding the drug's first-pass metabolism.

REFERENCE

I. Amarachinta, P. R., Sharma, G., Samed, N., Chettupalli, A. K., Alle, M., & Kim, J. C. (2021). Central composite design for the development of carvedilol-loaded transdermal ethosomal hydrogel for extended and enhanced anti-hypertensive effect. Journal of nanobiotechnology, 19, 1-15.

II. Jahangir, M. A., Anand, C., Muheem, A., Gilani, S. J., Taleuzzaman, M., Zafar, A., ... & Barkat, M. A. (2020). Nano phytomedicine based delivery system for CNS disease. *Current Drug Metabolism*, *21*(9), 661-673.

III. Beg, S., Al Robaian, M., Rahman, M., Imam, S. S., Alruwaili, N., & Panda, S. K. (Eds.). (2020). *Pharmaceutical drug product development and process optimization: effective use of quality by design*. CRC Press.

IV. Chettupalli, A. K., Ananthula, M., Amarachinta, P. R., Bakshi, V., & Yata, V. K. (2021). Design, formulation, in-vitro and ex-vivo evaluation of atazanavir loaded cubosomal gel. *Biointerface Res Appl Chem*, *11*(4), 12037-12054.

V. Unnisa, A., Chettupalli, A. K., Al Hagbani, T., Khalid, M., Jandrajupalli, S. B., Chandolu, S., & Hussain, T. (2022). Development of dapagliflozin solid lipid nanoparticles as a novel carrier for oral delivery: statistical design, optimization, in-vitro and in-vivo characterization, and evaluation. *Pharmaceuticals*, *15*(5), 568.

VI. Jahangir, M. A., Jain, P., Verma, R., Taleuzzaman, M., Ahsan, M. J., Chettupalli, A. K., ... & Mirza, M. (2022). Transdermal nutraceuticals delivery system for CNS disease. *CNS & Neurological Disorders-Drug Targets (Formerly Current Drug Targets-CNS & Neurological Disorders)*, *21*(10), 977-993.

VII. Kumar, A. C., Krishna, R. G., Venkanna, C. K., & Rafi, S. (2017). Formulation and characterization of itraconazole ethosomal gel for topical application. *J Bio Innov*, *6*, 55-64.

VIII. Bakshi, V., Amarachinta, P. R., & Chettupalli, A. K. (2022). Design, development and optimization of solid lipid nanoparticles of Rizatriptan for intranasal delivery: invitro & invivo assessment. *Materials Today: Proceedings*, *66*, 2342-2357.

IX. Jahangir, M. A., Muheem, A., Haque, M. A., Ananda, C., Taleuzzaman, M., & Kala, C. (2022). Formulation and Challenges in Liposomal Technology in Functional Food and Nutraceuticals. In *Liposomes for Functional Foods and Nutraceuticals* (pp. 165-195). Apple Academic Press.

X. Hemalatha, C. H., Vasavi, G., Kumar, A., & Sriram, N. (2014). Formulation and development of gliclazide microspheres for pharmaceutical evaluations. *Int J Adv Pharm*, *4*, 83-92.

XI. Dandamudi, S. P., Chettupalli, A. K., Dargakrishna, S. P., Nerella, M., Amara, R. R., & Yata, V. K. (2022). Response surface method for the simultaneous estimation of atorvastatin and olmesartan. *Trends in Sciences*, *19*(18), 5799-5799.

XII. Kanakagiri, D., & Chettupalli, A. K. (2022). Development of a transdermal delivery system for tacrine. *South Asian Res J Pharm Sci*, *4*(1), 6-16.

XIII. Pawar, P. M., Solanki, K. P., & Mandali, V. A. (2018). Recent advancements in transdermal drug delivery system. *Int J Pharm Clin Res*, *10*(3), 65-73.

XIV. Unnisa, A., Chettupalli, A. K., Alazragi, R. S., Alelwani, W., Bannunah, A. M., Barnawi, J., ... & Hussain, T. (2023). Nanostructured lipid carriers to enhance the bioavailability and solubility of ranolazine: Statistical optimization and pharmacological evaluations. *Pharmaceuticals*, *16*(8), 1151.

XV. Avula, P. R., Chettupalli, A. K., Chauhan, V., & Jadi, R. K. (2023). Design, formulation, in-vitro and in-vivo pharmacokinetic evaluation of Nicardipine-nanostructured lipid carrier for transdermal drug delivery system. *Materials Today: Proceedings*.

XVI. Kumar, T. S., & Chettupalli, A. K. (2015). Statistically optimized binary ethosomal gel of Carvedilol: allevialates hypertenstion in male Wistar albino rats. *Mol2Ne*, *1*, 1-20.

XVII. Chettupalli, A., Avula, P. R., & Chauhan, V. (2023). Improved Transdermal Delivery of Anti-hypertensive Drug Loaded Nanostructured Lipid Carriers: Statistical Design, Optimization, Depiction and Pharmacokinetic Assessment.

XVIII. Priya, S. S., Choudhury, A., Archana, N. K., Ananda, C., & Jahangir, M. A. (2023). Efficacy of Metallic Nanoparticles and Nanocarriers as an Advanced Tool for Imaging and Diagnosis: Insight into Theranostic Applications. *International Journal of Biomedical Investigation*, *6*(2), 1-17.

XIX. Sameina, L. H., Idamakantia, S., Chettupalli, A. K., Velamala, R. R., & Ezzat, M. O. (2023). Design of mesalamine loaded micro-particles: Preparation, in vitro and in-vivo characterization. *Materials Today: Proceedings*.

XX. Chettupalli, A. K., Ajmera, S., Amarachinta, P. R., Manda, R. M., & Jadi, R. K. (2023). Quality by Design Approach for Preparation, Characterization, and Statistical Optimization of Naproxen Sodium-loaded Ethosomes via Transdermal Route. *Current Bioactive Compounds*, *19*(10), 79-98.

XXI. Peddapalli, H., Sirigadi, M., Faheemuddin, M., Amara, R. R., & Chettupalli, A. K. (2021). Design, Development And Evaluation Of Antidiabetc Matrix Tablets Using Natural And Synthetic Polymers. *International Journal of Pharmaceutical Research (09752366)*, *13*(1).

XXII. Hussain, A. A. (1998). Intranasal drug delivery. Advanced Drug Delivery Reviews, 29(1-2), 39-49.

XXIII. Pontiroli, A. E. (1998). Peptide hormones: review of current and emerging uses by nasal delivery. *Advanced drug delivery reviews*, *29*(1-2), 81-87.

XXIV. Behl, C. R., Pimplaskar, H. K., Sileno, A. P., Demeireles, J., & Romeo, V. D. (1998). Effects of physicochemical properties and other factors on systemic nasal drug delivery. *Advanced drug delivery Reviews*, *29*(1-2), 89-116.

XXV. Illum, L. (2003). Nasal drug delivery—possibilities, problems and solutions. *Journal of controlled release*, *87*(1-3), 187-198.

XXVI. Illum, L. (2000). Transport of drugs from the nasal cavity to the central nervous system. *European journal of pharmaceutical sciences*, *11*(1), 1-18.

XXVII. Song, Y., Wang, Y., Thakur, R., Meidan, V. M., & Michniak, B. (2004). Mucosal drug delivery: membranes, methodologies, and applications. *Critical Reviews™ in Therapeutic Drug Carrier Systems*, *21*(3).

XXVIII. Belgamwar, V. S., Patel, H. S., Joshi, A. S., Agrawal, A., Surana, S. J., & Tekade, A. R. (2011). Design and development of nasal mucoadhesive microspheres containing tramadol HCl for CNS targeting. *Drug delivery*, *18*(5), 353-360.

XXIX. Chalikwar, S. S., Mene, B. S., Pardeshi, C. V., Belgamwar, V. S., & Surana, S. J. (2013). Self-

assembled, chitosan grafted PLGA nanoparticles for intranasal delivery: design, development and ex vivo characterization. *Polymer-Plastics Technology and Engineering*, *52*(4), 368-380.

XXX. Piao, H. M., Balakrishnan, P., Cho, H. J., Kim, H., Kim, Y. S., Chung, S. J., ... & Kim, D. D. (2010). Preparation and evaluation of fexofenadine microemulsionsfor intranasal delivery. *International journal of pharmaceutics*, *395*(1-2), 309-316.

XXXI. Ugwoke, M. I., Agu, R. U., Verbeke, N., & Kinget, R. (2005). Nasal mucoadhesive drug delivery: background, applications, trends and future perspectives. *Advanced drug delivery reviews*, *57*(11), 1640-1665.

XXXII. Qiang, F., Shin, H. J., Lee, B. J., & Han, H. K. (2012). Enhanced systemic exposure of fexofenadine via the intranasal administration of chitosan-coated liposome. *International journal of pharmaceutics*, *430*(1-2), 161-166.

XXXIII. Dhakar, R. C., Maurya, S. D., Tilak, V. K., & Gupta, A. K. (2011). A review on factors affecting the design of nasal drug delivery system. *International journal of drug delivery*, *3*(2), 194.

XXXIV. Kazi, K. M., Mandal, A. S., Biswas, N., Guha, A., Chatterjee, S., Behera, M., & Kuotsu, K. (2010). Niosome: a future of targeted drug delivery systems. *Journal of advanced pharmaceutical technology & research*, *1*(4), 374.

XXXV. Mahale, N. B., Thakkar, P. D., Mali, R. G., Walunj, D. R., & Chaudhari, S. R. (2012). Niosomes: novel sustained release nonionic stable vesicular systems—an overview. *Advances in colloid and interface science*, *183*, 46-54.

XXXVI. Moghassemi, S., & Hadjizadeh, A. (2014). Nano-niosomes as nanoscale drug delivery systems: an illustrated review. *Journal of controlled release*, *185*, 22-36.

XXXVII. Shahiwala, A., & Misra, A. (2002). Studies in topical application of niosomally entrapped nimesulide. *J Pharm Pharm Sci*, *5*(3), 220-225.